AIAA JOURNAL
Vol. 30, No. 11, November 1992

# Unsteady Turbulent Skin-Friction Measurement in an Adverse Pressure Gradient

Kirk J. Flittie* and Eugene E. Covert†
*Massachusetts Institute of Technology, Cambridge, Massachusetts 02139*

**A near-surface-mounted hot-wire shear gauge was designed, built, and installed in three locations on the upper surface of an NACA 0012 airfoil. The time constant of the gauge is essentially the same as a hot-wire anemometer, which implies that the gauge can measure turbulent shear stress. The skin friction at these three locations was measured over a reduced frequency range of 0–6.4 at two angles of attack (0 and 10 deg). The results show that the skin-friction coefficient well away from the separation point has a value essentially equal to the quasisteady value and a lag proportional to the reduced frequency when the reduced frequency is $\leq 1.25$.**

## Nomenclature

| | |
|---|---|
| $c$ | = airfoil chord |
| $c_f(x, t)$ | = local skin-friction coefficient, $\tau_w/\frac{1}{2}\rho U_0^2$ |
| $\bar{c}_f$ | = time mean or steady-state skin-friction coefficient, $\lvert\bar{\tau}_w/\frac{1}{2}\rho U_0^2\rvert$; see Eq. (2) |
| $H$ | = boundary-layer shape factor $[\delta^*/\theta]$ |
| $k$ | = reduced frequency, $\omega c/2U_0$ |
| $k_x$ | = streamwise reduced frequency, $\omega x/U_0$ |
| $Q$ | = phase velocity of external disturbance |
| $Re_\theta$ | = Reynolds number based on momentum thickness $\lvert\rho U_0\theta/\mu\rvert$ |
| $T$ | = period of excitation |
| $t$ | = time |
| $U_e$ | = local velocity just outside the boundary layer |
| $\bar{U}_e$ | = time mean external velocity |
| $U_0$ | = freestream velocity |
| $x$ | = distance along airfoil |
| $y$ | = distance normal to airfoil |
| $\alpha$ | = angle of attack |
| $\delta^*$ | = boundary-layer displacement thickness (mean or steady value) |
| $\Delta U_e$ | = amplitude of unsteady part of external velocity |
| $\Delta\tau_w$ | = amplitude of unsteady skin friction |
| $\eta$ | = nondimensional complex similarity parameter for flat-plate flows [see Eq. (10)] |
| $\theta$ | = boundary-layer momentum thickness (mean or steady value) |
| $\mu$ | = coefficient of viscosity |
| $\rho$ | = fluid mass density |
| $\tau_w$ | = skin friction |
| $\bar{\tau}_w$ | = local mean value of skin friction [see Eq. (2)] |
| $\phi$ | = phase angle |
| $\omega$ | = frequency of excitation, rad/s |
| $\lvert(\Delta\tau_w/\bar{\tau}_w)/(\Delta U_e/\bar{U}_e)\rvert$ | = normalized skin-friction amplitude |

## Introduction

LOCAL skin friction is one of the most difficult fluid mechanical parameters to measure because it is of the order of one-hundredth to one one-thousandth of the dynamic pressure and because effective measurement requires a small sensor as well as high sensitivity.

Many ingenious instruments have been designed to be small and sensitive, particularly for use in two-dimensional flow. These instruments range from direct reading skin-friction balances to inferential methods that sample the velocity profile near the wall (like Preston tubes) to correlations with local heat transfer through the use of wall mounted hot wires or hot film gauges. Another inferential method includes mass transfer at the wall. Nevertheless, none of these instruments provides useful data for unsteady flow.

If the flow is unsteady, all of the difficulties are magnified, particularly if the unsteady component is much smaller than the steady component of the flow. One of the most compelling problems in unsteady measurements is ensuring a proper frequency response. Thus, for example, the hot film gauge can be shown to have a lag due to the thermal properties of the wall on which it is mounted. These difficulties have been discussed most recently by Cook.[1] Detailed surveys and critiques of techniques for measuring skin friction can be found in the work of Hanratty and Campbell[2] and Flittie.[3]

In 1984, Houdeville et al.[4] made a major advance in which they reported an application of the hot film gauge arranged so that it was sensitive to unsteady skin friction without any of the aforementioned problems. They describe their instrument as follows:

> The sensitive element . . . is a quartz element supporting a thin conductive layer. . . . A cavity is provided in the gage [sic] body under the fiber. . . . The quartz fiber is tin soldered to the electrical connector pins and the length of the sensitive element is 1 mm. The fibers are the same as those used in type 55R gages [sic] made by the DISA company. The probe must be carefully assembled so that the upper generatrix of the fiber lies within, or better than 0.02 or 0.03mm of the skin plane. The purpose of the (0.8mm wide and 1.0mm deep) cavity under the sensitive element is to reduce thermal leakage into the skin and to enable more heating, as the film of adhesive can be no longer damaged.

Houdeville and co-workers demonstrated the usefulness of the gauge through tests conducted on an airfoil and a cylinder in steady flow, and unsteady flow (up to 60 Hz) on a flat plate with a zero pressure gradient.

To ensure the highest frequency response possible, we chose a 0.635-mm long hot wire, whereas Houdeville employs a hot film on a quartz fiber. Our sensor[2] operates on essentially the same principles as theirs.

Presented as Paper 91-0168 at the AIAA 29th Aerospace Sciences Meeting, Reno, NV, Jan. 7–10, 1991; received July 1, 1991; revision received May 8, 1992; accepted for publication May 8, 1992. 

*Research Engineer, Department of Aeronautics and Astronautics, 77 Massachusetts Ave.

†Professor, Department of Aeronautics and Astronautics, MIT Room 33-215, 77 Massachusetts Ave. Fellow AIAA.

In this paper, after a description of our gauge and after the error analysis, we will focus on the application of this instrument to measuring local unsteady skin friction in an adverse pressure gradient.

Our shear gauge (Fig. 1) consists of an aluminum tube of 0.156 in. o.d. and 0.125 in. i.d. filled with an endgrain birch substrate. Two steel mascot broaches 0.005 in. in diameter near their tip were ultimately located 0.025 in. (0.635 mm) apart. A 10% rhodium-90% platinum sensing wire 0.001 in. in diameter was soldered to the broach tips. The sensor wire was located at about $2y^*$, or about 0.001 in. above the surface plane of the gauge. The sensing wire is above a cavity 0.001 in. deep and 0.002 in. wide cut into the surface of the birch substrate. Because of its method of construction, this gauge can be calibrated before installation and can also be removed and reused.

Typical operating characteristics for the gauge are: resistive overheat ratio 1.2–1.5, output voltage range 0–2.5 V, frequency response: flat to a rolloff frequency of ~ 1000 Hz, and time constant 0.1 ms.

The error analysis was based on the assumption that all of the sources of error are described by Gaussian statistics. The error analysis provides the following estimates of uncertainties[2]:

1) Mean skin-friction coefficients = ± 6%.
2) Skin-friction amplitudes = ± 20% if $\Delta U_e/\bar{U}_e < 0.01$, ± 10% if $\Delta U_e/\bar{U}_e > 0.01$.
3) Skin-friction phase angles = ± 15 deg if $\Delta U_e/\bar{U}_e > 0.01$, ± 10 deg if $\Delta U_e/\bar{U}_e > 0.01$.
4) Mean boundary-layer velocities = ± 3% $\bar{U}_e$.
5) Unsteady velocity amplitude = ± 15% if $\Delta U_e/\bar{U}_e < 0.01$, ± 10% if $\Delta U_e/\bar{U}_e > 0.01$.
6) Unsteady velocity phase angles = ± 15 deg if $\Delta U_e/\bar{U}_e < 0.01$, ± 10 deg if $\Delta U_e/\bar{U}_e > 0.01$.

## Description of the Experiment and Data Processing

The geometric conditions for these tests are given in Refs. 2–4 and are repeated in the Appendix for convenience. The unsteady excitation is caused by the rotating ellipse, which is located below and behind the airfoil. The NACA airfoil was mounted as shown in the Appendix at $\alpha = 0$ and 10 deg, and a far and near ellipse location are denoted positions A and C. The airfoil angle of attack for the experiments reported here was set such that the surface pressure distribution matched those measured in Ref. 5. The unsteady velocity outside the boundary layer was measured by a constant current hot wire anemometer. This signal was assumed to be made up of the sum of a time average part, a periodic part with zero mean, and a remainder of zero mean that when significant was

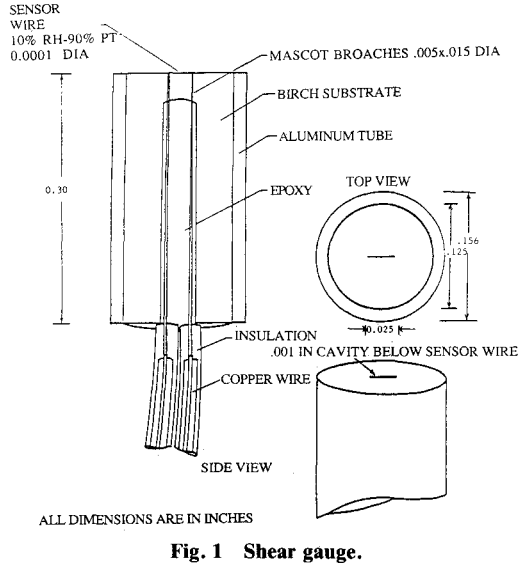


**Fig. 1 Shear gauge.**

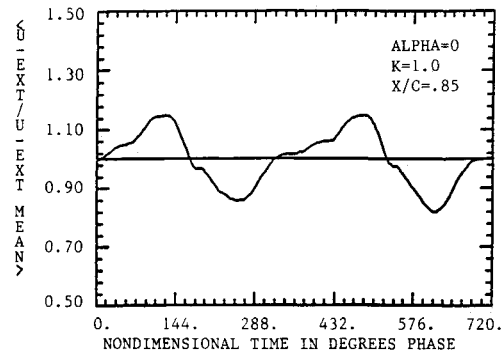


**Fig. 2 External velocity vs time.**

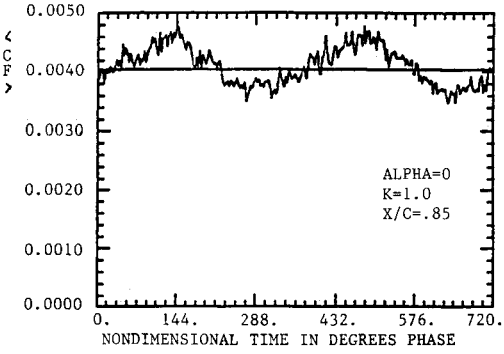


**Fig. 3 Typical skin-friction coefficient vs time.**

assumed to represent turbulence. If the directly measured signal is denoted as $u(x, t)$, the ensemble averaged signal is found as follows:

$$\langle u(x, t)\rangle = \frac{1}{N}\sum_{i=1}^{N} u(x, \omega t + iT + \phi) \tag{1}$$

The signal was also averaged with respect to time, i.e.,

$$\bar{u}(x) = \frac{1}{N}\sum_{i=1}^{N} u[x, \omega(t + i\Delta t) + \phi] \tag{2}$$

The unsteady part with zero mean is defined as

$$\tilde{u}(x, t) = \langle u(x, t)\rangle - \bar{u}(x) \tag{3}$$

The residual signal,

$$u'(x, t) = u(x, t) - \langle u(x, t)\rangle \tag{4}$$

is also of zero mean and is called "turbulence."

The raw signal was ensemble averaged until the next step made a change of <0.1%. This was about 500 cycles at the lowest frequency. At the highest frequency the ensemble average required up to 1000 cycles. The skin-friction coefficient was based on the mean freestream velocity. The zero reference angle was for the ellipse to be in the horizontal position (see Appendix). The phase of the excitation and the skin friction were measured with respect to this zero. Figures 2 and 3 show a typical waveform for the excitation and the skin-friction coefficient for the case of zero angle of attack, 0.70 chord, and $k = 1$. Note that the passage of time in these figures is denoted by the ellipse position and that two complete cycles are presented. The form of the excitation and the skin-friction coefficient were written as

$$\langle U_e(x, t)\rangle = \bar{U}_e(x) + \Delta U_e \cos(\omega t + \phi_u) \tag{5}$$

and

$$\langle c_f \rangle = \bar{c}_f(x) + \Delta c_f \cos(\omega t + \phi_\tau) \quad (6)$$

The ensemble averages were decomposed into the time mean and the first 10 harmonic components. The fluctuating signal in Fig. 3 has a frequency of 36 times the fundamental. The origin of this signal, which appeared in the skin friction and the inner layer velocity profile signal, is of a mechanical nature whose source is unknown. Except for this signal, the fundamental frequency dominated all of the data presented here.

## Steady Flow Turbulent Boundary-Layer Results

The results are presented in two parts: steady and unsteady skin-friction measurements. The skin friction was measured on the upper surfaces of an NACA 0012 airfoil at chord locations of 0.07, 0.85, and 0.94 chord. The chord Reynolds number was 700,000. The airfoil angle of attack is both $\alpha = 0$ and 10 deg. The results are given in Table 1, which also contains two estimated values of $c_f$.

At 0-deg angle of attack the estimated value of the skin friction was determined by two methods. One method was to use the formula of Ludweig and Tillman,[7] assuming local equilibrium and measured parameters, i.e.,

$$c_f = 0.246 \times 10^{-0.678H} Re_\theta^{-0.268} \quad (7)$$

This method agreed with the measurements to within 12%, with the largest error at higher values of $c_f$. The second procedure was to use the measured velocity profiles and curve fit them to determine the skin-friction coefficient using the law of the wall that Clauser[8] described. That is, each velocity profile corresponds uniquely to a given skin-friction coefficient. (These and other detailed data are given in Ref. 2.) The experimental values of the skin-friction coefficient agree with these estimated using Clauser's technique to ± 5% using a least-squares line. Note, too, that we have shown the experimental value of the root mean square of the fluctuating value of the skin friction [Eq. (4)] divided by the mean value of the skin friction. These values are smaller than those measured over a plate in a constant pressure field.

Table 1 also contains the measured values of the mean and fluctuating skin friction when the airfoil is inclined at an angle of attack of 10 deg. Clauser's method is not applicable here because the flow is so close to separation that the linear region in the law of the wall is vanishingly small.

In summary, the skin-friction data measured on the aft upper surface of an NACA 0012 airfoil are in good quantitative agreement with those determined by Clauser's method where it is applicable. We infer that the remaining data are also appropriate for the measuring conditions.

## Unsteady Turbulent Skin-Friction Results

Unsteady surface pressure measurements, unsteady velocity profiles, and skin friction were measured at the same positions and at reduced frequencies of 0.5, 1.0, and 1.25 for 0-deg

**Table 1 Steady turbulent boundary-layer parameters**

| Airfoil/ellipse orientation | $\alpha$/pos | $x/c$ | $\theta/c$ | $Re_\theta$ | $H$ | $c_f$ (Ref. 7) | $c_f$ (Ref. 8) | $c_f$ | $\sqrt{\left(\frac{\tau_w'}{\tau_w}\right)^2}$ |
|---|---|---|---|---|---|---|---|---|---|
| Airfoil alone | 0 | 0.70 | 0.0008 | 467 | 1.76 | 0.0035 | 0.0030 | 0.0032 | 0.10 |
| | | 0.85 | 0.0014 | 760 | 1.50 | 0.0048 | 0.0039 | 0.0047 | 0.07 |
| | | 0.94 | 0.0020 | 1279 | 1.47 | 0.0043 | 0.0038 | 0.0042 | 0.08 |
| Vertical ellipse | O/A | 0.85 | 0.0027 | 2072 | 1.47 | 0.0031 | 0.0032 | 0.0028 | 0.10 |
| | | 0.94 | 0.0056 | 2834 | 1.72 | 0.0020 | 0.0021 | 0.0019 | 0.10 |
| Horizontal ellipse | O/A | 0.85 | 0.0018 | 1217 | 1.41 | 0.0037 | 0.0038 | 0.0037 | 0.11 |
| | | 0.94 | 0.0022 | 1468 | 1.49 | 0.0034 | 0.0034 | 0.0036 | 0.12 |
| Vertical ellipse | 10/C | 0.85 | 0.0069 | 3702 | 1.78 | 0.0018 | | | 0.05 |
| | | 0.94 | 0.0078 | 4906 | 2.32 | 0.0010 | | | 0.04 |
| Horizontal ellipse | 10/C | 0.85 | 0.0133 | 9887 | 2.16 | 0.0008 | | | 0.03 |
| | | 0.94 | 0.0079 | 5096 | 2.32 | 0.0010 | | | 0.03 |

The correlation between Clauser's procedure and the data is $c_{f_{CL}} = 1.014 c_{f_m} + 0.00031 \pm 0.00024$.

**Table 2 Unsteady turbulent boundary-layer parameters for airfoil/ellipse configuration**

| $\alpha$/pos | $x/c$ | $k$ | $Re_\theta$ | $\bar{\delta}^*/c$ | $\bar{c}_f$ | $\Delta U_e/\bar{U}_e$ | $\frac{\Delta\tau_w/\bar{\tau}_w}{\Delta U_e/\bar{U}_e}$ | $\phi_{\tau_w} - \phi_{U_e}$ |
|---|---|---|---|---|---|---|---|---|
| O/A | 0.70 | 0.5 | — | 0011 | 0.0049 | 0.057 | 1.31 | −4 |
| | | 1.0 | — | 0011 | 0.0049 | 0.070 | 0.98 | 25 |
| | | 2.0 | — | 0011 | 0.0047 | 0.029 | 0.58 | 22 |
| | | 6.4 | — | 0011 | 0.0045 | 0.010 | 0.77 | 111 |
| O/A | 0.85 | 0.5 | 2716 | 0040 | 0.0040 | 0.025 | 3.98 | 6 |
| | | 1.0 | 1515 | 0030 | 0.0041 | 0.030 | 3.23 | 24 |
| | | 2.0 | 2212 | 0030 | 0.0037 | 0.009 | 2.04 | 11 |
| | | 6.4 | 1811 | 0036 | 0.0041 | 0.005 | 2.68 | 20 |
| O/A | 0.94 | 0.5 | 2133 | 0046 | 0.0030 | 0.032 | 5.56 | −7 |
| | | 1.0 | 2245 | 0054 | 0.0031 | 0.035 | 4.80 | 5 |
| | | 2.0 | 2199 | 0048 | 0.0030 | 0.014 | 4.38 | −10 |
| | | 6.4 | 1703 | 0042 | 0.0031 | 0.008 | 5.41 | −52 |
| 10/C | 0.70 | 0.5 | — | 0110 | 0.0019 | 0.110 | 2.87 | 14 |
| | | 1.0 | — | — | 0.0020 | 0.100 | 2.01 | 14 |
| | | 2.0 | — | — | 0.0018 | 0.042 | 0.71 | 32 |
| | | 6.4 | — | 0065 | 0.0021 | 0.060 | 0.99 | 147 |
| 10/C | 0.85 | 0.5 | 7769 | 0145 | 0.0018 | 0.040 | 6.80 | −7 |
| | | 1.0 | 5135 | 014 | 0.0018 | 0.040 | 4.17 | 16 |
| | | 2.0 | 4643 | 013 | 0.0016 | 0.010 | 4.26 | 6 |
| | | 6.4 | — | 0100 | 0.0021 | 0.012 | 1.11 | — |
| 10/C | 0.94 | 0.5 | 6824 | 024 | 0.0008 | 0.048 | 8.37 | 17 |
| | | 1.0 | 6808 | 024 | 0.0008 | 0.047 | 4.06 | 15 |
| | | 2.0 | 6680 | 0220 | 0.0008 | 0.017 | 3.42 | 6 |
| | | 6.4 | 6958 | 0175 | 0.0012 | 0.008 | 4.48 | 102 |

angle of attack. In addition, unsteady skin friction was measured for $x/c$ positions of 0.70, 0.85, and 0.94 at reduced frequencies of 0.5, 1.0, 2.0, and 6.4 and at $\alpha = 0$ and 10 deg. (These reduced frequencies correspond to periodic excitation of 6.2, 12.4, 24.8, and 79.4 Hz.) The mean skin-friction coefficient and the unsteady skin-friction coefficient amplitude and its phase are given in Table 2.

Measured velocity profiles were used to compare different techniques for calculating skin friction. Figures 4 and 5 show a comparison of quasisteady application of Ludweig and Tillman's formula and the Clauser process, as well as the equation of Cousteix et al.[9] for 0 deg angle of attack, at 0.85 and 0.94 stations. Again the general agreement between the data and the calculations is good. The unsteady velocity profiles at each instant in time reproduce the jagged curve of the skin friction faithfully for both angles of attack.

Lorber and Covert's data[3] show that the unsteady pressure distribution has the expected linear phase shift over a substantial fraction of the chord. Downstream of the 0.70 point there is a shift toward a constant phase situation. This is shown in Figs. 6 and 7 (from Ref. 5) and implies that the constant phase model is appropriate for interpreting the data in the region near the $x/c = 0.85$ point. For low unsteady excitation level, the data of both Lorber and Covert[10] and Patel[11] show that the mean velocity profiles in region of low or zero adverse pressure gradients are essentially the same as the steady-state velocity profiles at the same location.

It is of interest to compare that skin-friction amplitude and phase shift with other constant phase excitation unsteady data. For this comparison the length reduced frequency $\omega x/\bar{U}_e$ based on the distance from the leading edge was used. The primary purpose for this comparison is to determine what trends, if any, exist in unsteady skin friction as a function of reduced frequency. The data in Table 1 show that the 0-deg angle of attack steady data at $x/c$ is 0.85, and for both ellipse

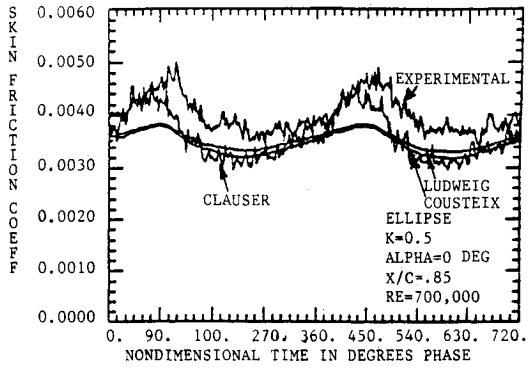


**Fig. 4 Normalized skin-friction coefficient vs time.**

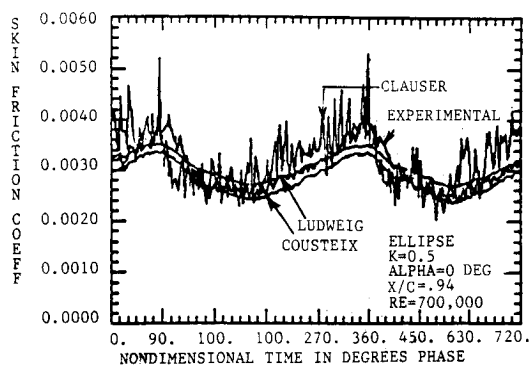


**Fig. 5 Normalized skin-friction coefficient vs time.**

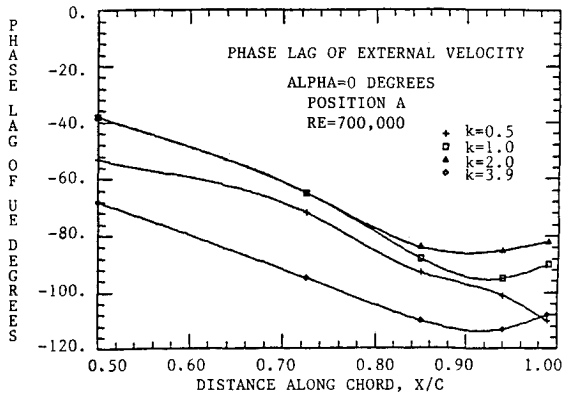


**Fig. 6 Excitation phase lag for several reduced frequencies ($\alpha = 0$ deg).**

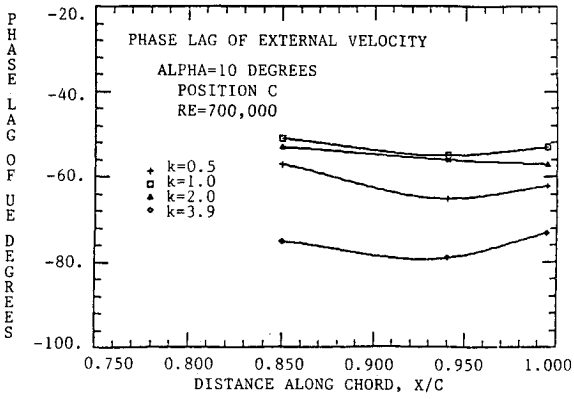


**Fig. 7 Excitation phase lag for several reduced frequencies ($\alpha = 10$ deg).**

positions when expressed in terms of boundary-layer parameters, may be considered to be approximately equivalent to flat-plate data. Figure 8 shows the normalized skin-friction amplitude at 0-deg angle of attack as compared with the flat-plate data of Cousteix et al.[9] The data at 0.85 and $\alpha = 0$ deg are in reasonable agreement with the data of Cousteix et al. Also shown in Fig. 8 are the unsteady data near the trailing edge. The data in Table 1 suggest that this point is much closer to the separation point. Thus, the unsteady excitation, not unexpectedly, has a stronger effect on the fractional change in the skin-friction coefficient. Figure 9 shows the phase shift for all of our data, the data of Cousteix et al., and additional data cited by Tellionis,[12] which is labeled to identify the original author. All experimental phase leads of the skin friction tend to lie between 0 and 40 deg. The data at $x/c = 0.85$, which are more or less constant phase points, are in good agreement with the other constant phase data. Patel's data[11] suggest that, for a wave speed of 0.77 of the freestream speed, the phase shift across the unsteady turbulent boundary layer is essentially zero at low reduced frequencies. Examination of the data taken at the 0.70 chordwise station shows a smallish value for the phase shift at lower reduced frequencies.

## Analysis

There is not a general theory that predicts unsteady skin friction. However, two special cases are available and can be used to help analyze this data. The first is due to Lighthill,[13] who studied the problem of predicting the unsteady laminar skin friction in a constant phase excitation. Later Patel[11,14] studied laminar and turbulent boundary layers subjected to a traveling wave excitation. Following the structure of

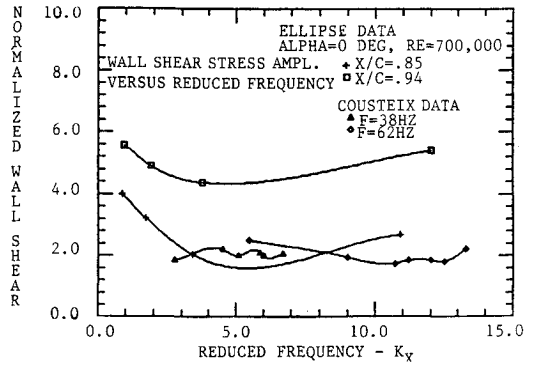


**Fig. 8 Normalized skin-friction coefficient vs $k_x$ at $\alpha = 0$ deg.**

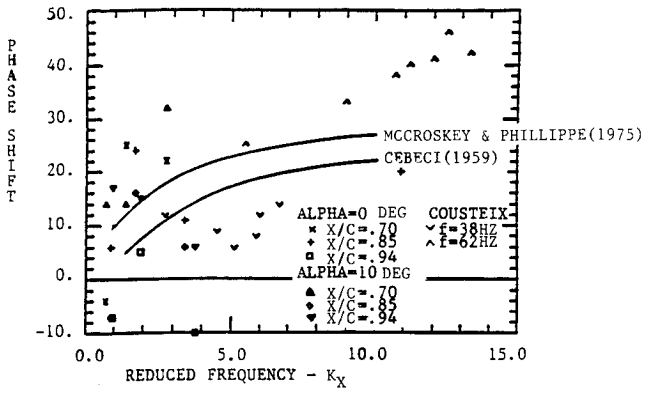


**Fig. 9 Wall shear stress phase shift.**

Lighthill's equation after generalization to fit Patel's result, we find

$$\mu\left(\frac{\partial u}{\partial y}\right)_w = \tau_w = \bar{\tau}_w + \frac{\Delta U_e}{\bar{U}_e}\left[\left(2 + \frac{\bar{U}_e}{\bar{c}_f}\frac{\partial \bar{c}_f}{\partial \bar{U}_e}\right)\bar{\tau}_w + i\left(\frac{1}{2} - \frac{\pi}{2}\frac{\bar{U}_e}{Q}\right)\frac{k\delta^*}{c}\right]e^{i\omega(t - x/Q)} \tag{8}$$

Equation (8) reduces to Lighthill's results for the case of a constant phase excitation of a laminar boundary layer on a flat plate. (Note that this follows if the phase velocity $Q$ becomes infinitely large.) Equation (8) also becomes a good approximation to Patel's approximate solution for unsteady laminar flow. As noted earlier, Patel and Lorber and Covert show that the mean velocity profiles in unsteady flow are essentially the same as the steady flow velocity profiles at the same conditions as the mean flow. The coefficient of the first term in the brackets is essentially the first term in an expansion about the mean flows. The second follows directly from the integrated form of the boundary-layer equation. Hence, it is valid to generalize the application of Eq. (8) directly to the turbulent boundary layers as well; thus, Eq. (8) is valuable as a basis for further discussion. Equation (8) is useful, particularly when reduced to a nondimensional form and specialized to a turbulent boundary layer over a flat plate for convenience. Thus,

$$c_f = \bar{c}_f + \frac{\Delta U_e}{\bar{U}_e}\left[1.8\bar{c}_f + i\left(\frac{1}{2} - \frac{\bar{u}}{2}\frac{\bar{U}_e}{Q}\right)\frac{k\delta^*}{c}\right]e^{i\omega(t - x/Q)} \tag{9}$$

Equation (9) provides a way of interpreting the fractional change in the skin friction normalized with respect to the fractional change in the velocity as given in Table 2 and Figs. 4, 5, and 8. This is a reasonable normalization, since Patel[11] has shown earlier that, for small amplitudes of the unsteady excitation, the process is essentially linear. Let $\eta$ denote the complex term in the brackets. The $\eta$ is a parameter that illustrates the nature of the unsteady skin-friction results. After suppressing the exponential time factor, $\eta$ takes the following form for a flat plate:

$$\eta = 1.8 + i\left(\frac{1}{2} - \frac{\pi}{2}\frac{\bar{U}_e}{Q}\right)\frac{k\delta^*}{\bar{c}_f c} \tag{10}$$

Equation (10) shows that similarity is possible if and only if

$$\left(\frac{1}{2} - \frac{\pi}{2}\frac{\bar{U}_e}{Q}\right)\frac{\delta^*}{\bar{c}_f c}$$

is constant. In that case $\eta$ will reduce to a single curve as a function of $k$. The data scatter in Fig. 9 indicates that these flows are far from being in a similar state. Equation (10) also shows that the imaginary part will dominate $\eta$ when $k$ is large or when $\bar{c}_f$ or $Q$ is small. Although this analysis is probably not valid as $\bar{c}_f$ nears zero, the approximation points out that the imaginary part of $\eta$ becomes large as a separation point is approached. The data given in Table 2 can be used to estimate the value of $\eta$. At $\alpha = 0$ deg the calculated value of $\eta$ agrees roughly with the data at station 0.85. At station 0.94 the magnitude of $\eta$ that is calculated is about half the experimental value. This is due to the difficulties in determining the value of the derivative $(\partial \bar{c}_f/\partial \bar{U}_e)$. In both cases the increase in the phase angle with $k$ is qualitatively correct. Thus, one concludes that Eqs. (8–10) provide a rational means of interpreting the unsteady skin-friction data.

## Conclusions

The results and conclusions are as follows:

1) The skin-friction gauge described herein provides unsteady turbulent skin-friction data in an adverse pressure gradient, as given in Tables 1 and 2.

2) The skin-friction gauge provides values of skin friction that agree well with those determined by use of the unsteady velocity profiles that exhibit a satisfactory "law of the wall" region for the values of reduced frequency of 1.25 or less.

3) An elementary formula [Eq. (9)] illustrates the conditions necessary to define similarity in these complex unsteady flows.

4) Despite a lack of detailed similarity, the normalized skin-friction data show a well-behaved behavior with $k$ in uniform and adverse pressure gradients.

## Appendix: NACA 0012 Airfoil/Ellipse Test Configuration

The experimental apparatus used to study unsteady turbulent boundary layers was identical to that used by Lorber and Covert[5] in earlier experiments and is shown in Fig. A1. The details of this experimental arrangement have also been discussed recently in Ref. 6. An NACA 0012 airfoil was mounted stationary between two plywood vertical sidewalls to ensure two-dimensional flow on the airfoil. An elliptic cylinder was used to generate a nearly constant phase unsteady upwash on the airfoil, which results in traveling disturbance just outside the boundary layer. Details of the flowfield induced by the ellipse with and without the airfoil present in the test section can also be found in Refs. 5 and 6. A diagram of the airfoil/ellipse configuration is shown in Fig. A1.

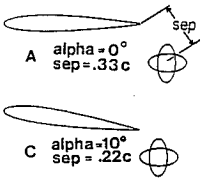


**Fig. A1 NACA 0012 airfoil and elliptic cylinder positions.**

## Acknowledgments

This research was conducted in part under Air Force Office of Scientific Research (AFOSR) Contract F49620-79-0226 and AFOSR Grant 81-0282. Michael Francis, USAF, was the technical monitor. The astute reader will note that Ref. 4 was not included in our AIAA 1991 Science Meeting preprint (91-0168). We want to thank R. Houdeville for calling our attention to that publication, which was somehow overlooked in the preparation of our 1991 preprint.

## References

[1]Cook, W., "Response of Hot Element Shear Stress Gages in Unsteady Turbulent Flows," AIAA Paper 91-0167, 1991.

[2]Hanratty, T. J., and Campbell, J. A., "Measurement of Wall Shear Stress," *Fluid Mechanics Measurements,* edited by R. J. Goldstein, Hemisphere, New York, 1983.

[3]Flittie, K. J., "Wall Shear Measurements in an Unsteady Turbulent Boundary Layer," M.S. Thesis, Dept. of Aeronautics and Astronautics, Massachusetts Inst. of Technology, Cambridge, MA, Sept. 1985.

[4]Houdeville, R., Jullien, J. C., and Cousteix, J., "Skin Friction Measurements with Hot Element Gages," *La Recherche Aerospatiale,* 1984, Vol. 1, pp. 67–79.

[5]Lorber, P. E., and Covert, E. E., "Unsteady Airfoil Pressures Produced by Periodic Aerodynamic Interference," *AIAA Journal,* Vol. 20, No. 9, 1982, pp. 1153–1159.

[6]Covert, E. E., Phillips, S. M., and Vacy, C. M., "Deep Stall of an NACA 0012 Airfoil Induced by Periodic Aerodynamic Interference," *ASME FED International Symposium on Nonsteady Fluid Dynamics,* Vol. 92, edited by J. A. Miller and D. P. Tellionis, American Society of Mechanical Engineers, New York, Book No. 1597-1990.

[7]Ludweig, H., and Tillman, W., "Instrument for Measuring the Wall Shearing Stress of Turbulent Boundary Layers," NACA TM 1284, 1950.

[8]Clauser, F. H., "Turbulent Boundary Layers in Adverse Pressure Gradients," *Journal of the Aeronautical Sciences,* Vol. 21, No. 2, 1954, pp. 91–108.

[9]Cousteix, J., Houdeville, R., and Janvelle, J., "Response of a Turbulent Boundary Layer to a Pulsation of the External Flow with and without Adverse Pressure Gradient," *Unsteady Turbulent Shear Flows,* Springer-Verlag, Berlin, 1981.

[10]Lorber, P. F., and Covert, E. E., "Unsteady Turbulent Boundary Layers in Adverse Pressure Gradients," *AIAA Journal,* Vol. 22, No. 1, 1984, pp. 22–28.

[11]Patel, M. H., "On Turbulent Boundary Layers in Oscillatory Flow," *Proceedings of the Royal Society of London, Series A,* Vol. 353, 1977, pp. 121–137.

[12]Tellionis, D. P., *Unsteady Viscous Flows,* Springer-Verlag, New York, 1981, pp. 186–276.

[13]Lighthill, M. J., "The Response of Laminar Skin Friction and Heat Transfer to Fluctuations in the Stream Velocity," *Proceedings of the Royal Society of London, Series A,* Vol. 224, 1954, pp. 1–23.

[14]Patel, M. H., "On Laminar Boundary Layers in Oscillatory Flow," *Proceedings of the Royal Society of London, Series A,* Vol. 347, 1975, pp. 99–123.